Tellus (2008), 60B, 405–415
Printed in Singapore. All rights reserved

TELLUS

Chemical properties of Arctic aerosol particles collected at the Zeppelin station during the aerosol transition period in May and June of 2004

By ULRIKA BEHRENFELDT[1], RADOVAN KREJCI[2], JOHAN STRÖM[1]* and ANDREAS STOHL[3], [1]*Department of Applied Environmental Science, Stockholm University, S-106 91 Stockholm, Sweden;* [2]*Department of Meteorology, Stockholm University, S-106 91, Stockholm, Sweden;* [3]*Norwegian Institute for Air Research, NILU, Norway*

(Manuscript received 11 October 2007; in final form 26 February 2008)

ABSTRACT

Single particle analysis was performed on samples taken at the Zeppelin Station, Svalbard, during the ASTAR campaign, 2004. Thirteen samples were selected to representatively cover the campaign period and different weather conditions. This particular period also covers the transition from an accumulation mode dominated size distribution in spring to an Aitken mode dominated aerosol size distribution in summer. Altogether, 1353 particles were analysed and their elemental composition documented. Another 1225 were counted but not characterized chemically. The samples were compared with respect to chemical composition, aerosol size, shape and airmass origin. The comparison showed that the samples taken before the aerosol size transition were dominated by spherical 'organic like' particles in the submicrometre range, with an Eurasian influence. The samples taken after the size transition showed a more complex character and the source origin was the Arctic basin. In this period, an increase of both marine aerosol groups as well as groups of continental origin became more pronounced. This apparent contradiction may have its explanation in cloud scavenging processes, removing the hygroscopic particles from the old continental air, leaving the more hydrophobic particles, at the same time, as the ocean source will provide a more maritime character.

1. Introduction

The Arctic is a very vulnerable ecosystem, sensitive to even small changes in the climate. On a global scale, climate models predict the largest increase of the annual mean temperature to occur in the Arctic, which is also supported by observations (ACIA, 2005). Due to the large sensitivity and pristine background conditions, the evolution of the Arctic climate can be seen as an early warning for possible climate changes on a global scale.

Over the last 40 yr, the focus, with respect to pollution and aerosols in the Arctic, has been on the Arctic Haze. This phenomenon was first noted in the literature by Mitchell (1957) and occurs usually during late winter and early spring. As a result of the numerous experiments and measurements, it has been shown that the Arctic Haze is predominantly of anthropogenic origin from lower latitudes, especially from the Eurasian continent (Heintzenberg and Larssen, 1983; Beine, 1999; Sirois and Barrie, 1999; Quinn et al., 2002). In contrast to the Arctic Haze period, the summer months are much cleaner due to stronger blocking of the pollutant transport into the Arctic and weaker source strength due to less domestic heating.

In agreement with the established climatologies of the mean pressure distribution in the Arctic region (cf. Liljequist, 1970), Eneroth et al. (2003) found that for the years 1992–2001, the most common transport pathways to Ny-Ålesund in winter were associated with the North Atlantic storm track, making the North Atlantic and Eurasia the source regions. During spring, the source regions were located closer to the Arctic, predominantly over Northern Greenland, the North Atlantic, Scandinavia and the area surrounding Svalbard. The summer months showed a similar pattern, and the Eurasian influence was further suppressed. Koch and Hansen (2005) suggested that emissions from South Asia, together with biomass burning emissions could be a significant source of black carbon to the Arctic in the summer time. However, Stohl (2006) presented numerical simulations indicating this pathway to be unlikely.

The atmospheric aerosol affects the climate both directly and indirectly. The direct effect is through absorption and scattering of radiation. The exact nature of how the aerosol is scattering or absorbing light depends on its shape, size and chemical

*Corresponding author.
e-mail: johan@itm.su.se
DOI: 10.1111/j.1600-0889.2008.00349.x

composition. The indirect effect considers the aerosol's ability to act as cloud condensation nuclei (Charlson et al., 1992) and thereby influence the cloud microphysical and optical properties, as well as cloud lifetime (Rosenfeld, 2000). Whether a cloud serves to warm or cool the Earth's surface depends on the altitude and thickness of the cloud as well as on the surface albedo and the solar zenith angle. The net radiative effect of the Arctic aerosol depends on the complex interaction between the aerosols, clouds, surface albedo and transport processes. However, it is suspected that specific interactions between solar radiation, low solar zenith angle, high surface albedo, aerosol particles and clouds magnify the radiative impact of the atmospheric aerosols in the Arctic region (Quinn et al., 2002).

Other important factors affecting the aerosol lifetime in the Arctic are precipitation and insolation. Low precipitation rate, together with a stable thermal stratification of the atmosphere in winter, gives the aerosol time to age and grow (Baskaran and Shaw, 2001). In summer, extensive cloud cover and precipitation act to clean the air from pollutants and remove much of the aerosol introduced to the Arctic.

From a 1 yr analysis of Arctic aerosol properties, Ström et al. (2003) showed that the aerosol size distribution at the Zeppelin station, Svalbard, undergoes a very rapid transition in its characteristics between the spring and summer period. The aerosol size-distribution changes from being accumulation mode dominated to an Aitken mode dominated distribution over only a few days. Engvall et al. (2007) showed from a compilation of 6 yr of data that this is a feature that repeats itself from year-to-year within a time window of approximately 2 weeks. The authors concluded that the changes in air mass origin are an important pre-requisite, but it cannot alone explain the repeated spring-summer aerosol size transition.

Using single particle analysis, this study investigates if similar change can be observed also in aerosol chemical composition and what major aerosol types are observed in the Arctic during spring and early summer period. We formulate this into three specific questions:

- Can we observe differences in aerosol composition and mixing state between samples representing spring and summer Arctic aerosol?
- What are the major groups of the aerosol particles based on their elemental composition, shape and size?
- Can we address main source regions of aerosol particles using the result of single particle analysis and air mass history?

2. Methodology

2.1. Sample collection

The samples for single particle analysis used in this study were taken in the second half of May and first half of June 2004, at the Zeppelin Research Station, Svalbard, during the Arctic Study of Tropospheric Aerosols, Clouds and Radiation (ASTAR 2004) campaign. The station is situated on a mountain ridge, 474 m above sea level. Due to its location, the station is practically unaffected by local sources, and since the station is mostly below the boundary layer cloud top, the observations at the station are regarded as representative for boundary layer conditions (Ström et al., 2003). The Department of Applied Environmental Science (ITM) at Stockholm University and the Norwegian Institute for Atmospheric Research (NILU) are the main users of the station for continuous measurements.

Through 100 mm diameter shaft, covered from rain, the air is lead through the roof into the building. The transport through the approximately 5 m long pipe and a total volume flow of approximately 30 L min^{-1} gave a transport time of the sample air of about 5 min. From the shaft a 1/4 inches pipe of stainless steel of length about 1.5 m takes the sample air to the filter holder. The flow rate through the stainless tube was 1.7 L min^{-1}. Nuclepore polycarbonate membrane filters with pore diameter 0.4 μm where used as substrate. A Teflon plate, with a hole, supported the filter from below, and the active sampling area was, thereby, reduced to 7 mm in diameter. This was done to enrich particle concentration to a limited area, which facilitates the analysis with the Scanning Electron Microscope (SEM). The sample airflow was controlled using a critical orifice, and the volume of air passing the filters was constant. Each filter was exposed for 6 h.

Over 50 samples were collected during the campaign. For this study, 13 filters were selected to representatively cover the whole campaign period and different weather conditions, such as clear sky, before cloud and in cloud. Due to the design of a rain-covered shaft, hydrometeors with a settling velocity greater than 0.5 cm s^{-1} (approximately 10 to 15 μm diameter) will be sampled with a low efficiency.

2.2. Filter preparation

After sampling the filters were stored in clean Petri dishes. Prior the analysis, the 7 mm in diameter exposed part was cut out and mounted on a specimen Al-stub using a conductive double-sided adhesive tape. All preparation work was done in a clean flow box. As a next step, the filters were coated with a thin layer of carbon to make them conductive. Another alternative could have been to use a gold sputter and coat the specimen with gold. Gold is in many ways better since it is more stable, oxidizes less and it is easier to coat the sample with a homogeneous micro layer. However, the X-ray L emission lines for gold coincide with K emission lines for sulphur, and as the sulphur distribution in aerosol particles is of interest for this study, carbon coating was more favourable. Moreover, the filters are made of polycarbonate, so light elements in aerosol particles, including carbon, cannot be measured directly.

2.3. SEM analysis

Single particle analysis was performed at the Department of Geology and Geochemistry, Stockholm University, using a modern Environmental Scanning Electron Microscope, ESEM Philips FEG 30XL, equipped with EDAX. The analyses were done at high vacuum mode. The electron acceleration voltage was set to 20 keV, and the spot size adjusted so that the X-ray counts per second was kept in the range of 700–800. The X-ray detector consisted of a windowless Si (Li) detector with a spectral resolution of 157 eV at 5.9 keV (Mn K_α). The detector was calibrated on a regular basis using Al–Cu standard. The instrument itself allows analysis of light elements ($Z > 5$), but due to the coating of the sample with carbon and the nature of the polycarbonate filter, only elements with $Z > 10$ (from Na) were considered in the X-ray spectra evaluation (Krejci et al., 2005).

The particles selected for elemental analysis were selected manually, based on the secondary electron image. The analysis started in the middle of the sample and then continued along a chosen direction. When the edge of the specimen was reached, the sample was again centred and the analysis continued along a new direction. All the particles encountered were analysed or, in the case of high number density of identical particles, counted. Regardless of size or shape, the maximum width and perpendicular length of each particle was measured, and the calculated mean value represents the particles diameter. The instrumental set-up and the electron microscope limitations of the size detection set the minimum particle size detection limit to approximately 0.1 μm in diameter. In this study, the particles will be divided into sub- or supermicrometre groups, based on their size defined above. Also a blank filter, treated the same as the other filters in all aspects, but the exposure to sampled air was excluded, was analysed to establish the degree of possible contamination.

Limitation of the SEM–EDX technique is that volatile material will evaporate in high vacuum inside of the SEM chamber. This may cause some particles to shrink or deform or even disappear completely. Particles, potentially affected by this, problem have not been treated in any specific way as part of the analysis. Therefore, the abundances of certain groups presented should be seen as upper limit, assuming that certain particles could volatilize in high vacuum. High-energy electron beam can cause further damage or deformation on aerosol particles during EDAX analysis. The size and shape of the aerosol particles was measured prior the EDAX analysis. The damage on the particles did not show any clear quantitative or qualitative pattern which could have been used in consecutive data analysis and interpretation. This aspect is not taken further into account.

2.4. Analysed and counted particles

In average 120 particles were analysed per filter, except for four filters where the number density of identical particles was high. For those filters, a frame was chosen and some of the identical particles (with respect to size and shape), within the frame, were analysed and the rest counted. Altogether, 1353 particles were analysed and another 1225 counted but not characterized chemically. In Table 2 is listed the abundance for each particle group per filter ± 1 *SD* calculated using equations from Ebert et al. (2000).

$$\sigma = \sqrt{N\ p_i\ (1 - p_i)}, \quad \text{where } p_i = \frac{\mu_i}{N}, \tag{2.4.}$$

N represents the total number of analysed particles, p_i the probability for a particle to fall into group i and μ_i stands for the absolute number of particles in group i.

There is no doubt that more analysed particles would have given a statistically better representation of each sample. On the other hand, single particle analysis performed on a non-automated instrument, like in this case, is very time demanding. Targino et al. (2006) performed statistical tests analysing around 150 particles twice from different parts of the same sample using the same instrument as in this study. The analysis showed that the abundance of defined particle groups indeed changed, but the big picture and the main fractions between defined groups remained the same. Thus, we believe that the number of particles analysed per sample in this study is an acceptable compromise between the analytical time needed and a sufficient quantity to obtain a representative result.

3. Results

3.1. Particle groups

Based on the results of the elemental composition and morphology analysis, particles were divided into eight groups. Some of the main groups were later divided in subgroups, where it was meaningful with respect to data interpretation. The main parameter used in the grouping process is elemental composition, but aerosol morphology, possible origin of the aerosol particles and processes they undergo in the atmosphere were also taken into account. Table 1 shows the main groups and their selection criteria.

3.1.1. Mineral dust (29 particles analysed). This group typically comprises of particles whose origin can be derived from the Earth's crustal surface. The most common type was Si-rich particles, but Fe-rich particles and Al-silicates with Na, Mg, Ca and K were also found. So, a possible aggregation between mineral dust and sea salt particles could have taken place. Four of the Si-rich particles were spherical and the rest had an irregular shape, whereas the division in size, between super- and submicrometre, were 12 and 17, respectively. In the case of spherical Si-particles, it cannot be completely excluded that these are ash particles since they are often spherical, and besides carbon, they can also contain certain amount of Si.

3.1.2. Aged mineral dust (83 particles analysed). Similar particles to those belonging to the previous group, but in addition, sulphur was detected. Another difference is that 12 of the particles in this group had Ca as the dominating element. The presence of

Table 1. The eight aerosol groups used for data interpretation, their dominating elements and characteristics

Group	Dominating elements	Characteristics
Mineral dust	Si, Fe, Al	Irregular
	(Na, Mg, Ca, K)	Possible aggregation of mineral dust and sea salt
Aged mineral dust	Si, Fe, Al, Ca	Irregular
	(Na, Mg, Ca, K) associated with S	Possible aggregation of mineral dust and sea salt
Sea salt	Na–Cl	Na–Cl: angular, supermicron
	Na	Na: submicron
Aged sea salt	Na–Cl, S	Na–Cl, S: angular, supermicron
	Na, S	Na, S: submicron
Undefined-Organic	Background signal, no elements detected	Divided into: Smooth
		Irregular
		Soot
Undefined-Organic + S	Background signal, S	
Undefined-Organic + X	Background signal Na, S	Weak emission lines
Mixed	Na, Mg, Ca, K, Al, Si, Fe, S	Equal dominance of elements associated with Sea salt and Mineral dust

sulphate indicates that the particles have been in the atmosphere for some time, and have gained the sulphate either through cloud processing or through heterogeneous oxidation of SO_2. More than 60%, or 53 particles, had a supermicrometre diameter, and 30 particles were in the submicrometre range. Only four were of spherical shape.

3.1.3. Sea salt (26 particles analysed). This group contains particles dominated by Na and Cl. Of these particles, 14 consisted of Na and Cl only. Some of them also contained magnesium. They were all crystalline shaped, most of them cubical, and with the exception of one, they were all in supermicrometre size range. The remaining 12 particles in this group had Na as the only detected element or, as in two cases, with a small addition of magnesium. One reason for the lack of Cl can be the chemical transformation of HNO_3 that would leave only Na as detectable signal. Five of the Na-particles were oval or rod shaped, while the rest were irregular, and with the exception of one, they all were a submicrometre diameter.

3.1.4. Aged sea salt (77 particles analysed). The main characteristics of the sea salt group above is that particles are dominated by Na and/or Cl. This is true for the aged sea salt particle group as well, but they also carried sulphate and in some cases small amounts of other elements like Mg, Al, Ca, K and Si. Almost 50% or 37 of the particles contained Na and Cl, most of them had shapes that suggest they were crystalline and only one was in the submicrometre range. The remaining 40 particles formed the subgroup 'Na + S', as they did not contain detectable amounts of Cl. The lack of Cl and presence of S points toward aged particles, where Cl has been released from the particle and S has been gained through acid displacement (Adams and Cox, 2002). Most of these particles were irregular and 31 had a mean diameter in the submicrometre range.

3.1.5. Undefined-Organic (636 particles analysed). This is the largest group in terms of frequency of particles, and it consists of particles that did not contain significant amounts of detectable elements with $Z > 10$ in the EDAX spectra. Though it is possible to identify elements lighter than Na, it is difficult to distinguish between C-O-N peaks from the polycarbonate filter, C peaks from the carbon coating and lighter element peaks from the particle. Spectra of this kind, with only background signal, have been described in the literature as typical for organic and biological material (e.g. Mamane and Noll, 1985; Xhoffer et al., 1991). Possible particles belonging to this group can be soot, fly ash, biological particles and ammonium nitrate. We are not aware of any measurements in the Arctic showing abundance of the ammonium nitrate in the atmospheric aerosol, which can explain presence of this group of particles. Thorough discussion of this issue is presented also in Krejci et al. (2005). One way of distinguishing between them is through their morphology. However, within the timeframe of this study, only a quantitative evaluation of the morphology could be done. Therefore, the group was divided into three subgroups: 'Smooth' (306) including spheres, elliptic and other simple smooth geometric shapes; 'Irregular' (284) and (possible) 'Soot like' (36). Another 1145 particles were counted, and added to the analysed ones for statistical calculations.

3.1.6. Undefined-Organic + S (86 particles analysed). Same as the undefined-organic group above, except for detectable emission lines of S. It is possible that these particles have biological origin. Observations claim that biological particles (composed of light elements such as hydrogen, carbon, oxygen and nitrogen) with their complex morphology and wet surfaces provide suitable nucleating surface for SO_2 absorption and conversion to sulphate, as well as deposition of submicrometre sulphates on the surface of these particles (Mamane and Noll, 1985). Another explanation can be that particles from this group spent longer time in the atmosphere, and deposition processes and in-cloud processing resulted in increased abundance of sulphur. For this group 80 additional particles were counted, and added to the analysed ones for statistical calculations.

3.1.7. Undefined-Organic + X (312 particles analysed). This is the second largest group, and as the previous two undefined-organic groups, its origin is somewhat unclear. The X-ray spectra for these particles show background signal and weak emission lines for Na or Na and S. A few particles in this group also carried magnesium, potassium and calcium.

3.1.8. Mixed (90 particles analysed). The particles in this group showed various combination of Na, Mg, Al, Si, S, Ca, K and Fe. Some of them showed only weak emission lines in the X-ray spectra; so, the presence of organic materials is also a possibility. Aggregation and ageing of aerosols in the atmosphere (e.g. through cloud processing) may result in these kinds of particles.

3.1.9. Contaminants. On the blank filter, we observed very few particles, considering that a much larger area was searched than on the other filters. The 29 particles, which were found, were almost transparent, and therefore very hard to spot. Eight of the blank filter particles contained chromium, and formed the group 'Cr^+'. The X-ray spectra, for these particles, show background signal with weak emission lines for Na, Mg, Si, S and Cr. Chromium is a known artefact for nuclepore polycarbonate filters and 'Cr^+' was thus treated as a contaminant on the sample filters. A total of 11 chromium particles where found on the sample filters compared with nearly 1400 analysed particles. However, 10 of these 'Cr^+' particles where observed on samples collected when the air came from Northern Russia. Thus, it is possible that some particles treated as contaminants where actually from anthropogenic sources. All the chromium particles were irregular and in the supermicrometre range.

The remaining non-chromium particles observed on the blank filter where divided as follows: Undefined-Organic (12); Undefined-Organic+ (3); Mineral dust (3); Aged mineral dust (3) and Mixed (1).

There were also two particles, on the sampling filters, that did not fit into any group; one was dominated by titanium (A6), and the other by iron and zinc (E6).

3.2. Air mass history

To investigate the origin of the air masses and source regions for the samples taken at the Zeppelin station, atmospheric backward transport simulations were made every 3 h, using the Lagrangian particle dispersion model FLEXPART (Stohl et al. 1998, 2005)—see http://zardoz.nilu.no/~andreas/STATIONS/ZEPPELIN/index.html. The model was driven with 1° resolution operational analysis data from the European Centre for Medium-Range Weather Forecasts. The model calculates the trajectories of so-called tracer particles using the mean winds interpolated from the analysis fields plus random motions representing turbulence and moist convection. Removal processes were not considered in the simulations.

The output of FLEXPART in backward mode is a potential emission sensitivity (PES) function. The word 'potential' indicates that this sensitivity is based on transport alone, ignoring removal processes that would reduce the sensitivity. The value of the PES function (in units of s kg^{-1}) in a particular grid cell is proportional to the particle residence time in that cell. It is a measure for the simulated mixing ratio at the receptor that a source of unit strength (1 kg s^{-1}) in the respective grid cell would produce. We show plots of the PES in a so-called footprint layer, extending from the surface to 100 m above which show where the air mass was likely in contact with the surface, since emissions of trace gases and aerosols mainly take place near the ground.

Folding (i.e. multiplying) the PES footprints with the emission flux densities (in units of kg m^{-2} s^{-1}) from an emission inventory (we use the EDGAR 3.2 fast track inventory for the year 2000; see Olivier and Berdowski, 2001) yields so-called potential source contribution (PSC) maps, which show the geographical distribution of contributing sources. Spatial integration finally gives the simulated mixing ratio at the receptor, which can be plotted as a time-series at the station and as a function of the 'age' of the emission.

Four situations were chosen to exemplify the major differences in pathways and source regions between the sampling dates.

(1) **22 and 23 May** (A4, A5, A6, A7), upper left-hand side picture, Fig. 1.

The first set of samples was collected during 24 h between 22 and 23 May. Air mass origin was similar for all four samples. The FLEXPART model shows the main source regions to be the Northern Russian tundra. It also shows that a spiral formed area, starting at the pole and turning clockwise over the Beaufort Ocean, Siberia and Scandinavia, can be regarded as the source regions, where the air mass was in contact with the ground. The FLEXPART age spectra for the trace gases SO_2, NO_2 and CO for this day show the European continent (mostly western Russia) to have the largest influence. Two of the particles found on filter A4 and eight on filter A7 carried chromium. When considering the source region, it is possible that these particles came from one of the Russian metal smelters in that region—FLEXPART PSC maps indicate the largest SO_2 contributions from the smelters on the Kola peninsula and in Norilsk. However, similar particles were also found on the blank filter, and since chromium is a known artefact for nuclepore polycarbonate filters, interpretation of the source for Cr^+ particles found on filters A4 and A7 must be done with caution.

(2) **27 May** (C1), **3 June** (E4, E5, E6), upper right-hand side picture, Fig. 1.

The main difference from the previous sampling occasion is that for these filters, the source region is the ice covered Arctic Ocean. The uptake area is also 'smeared out', in contrast to the narrow, almost straight pathway that could be observed for 22 and 23 May.

When going from 27 May to 3 June, there is also a shift in the main source region, from Svalbards closest surroundings

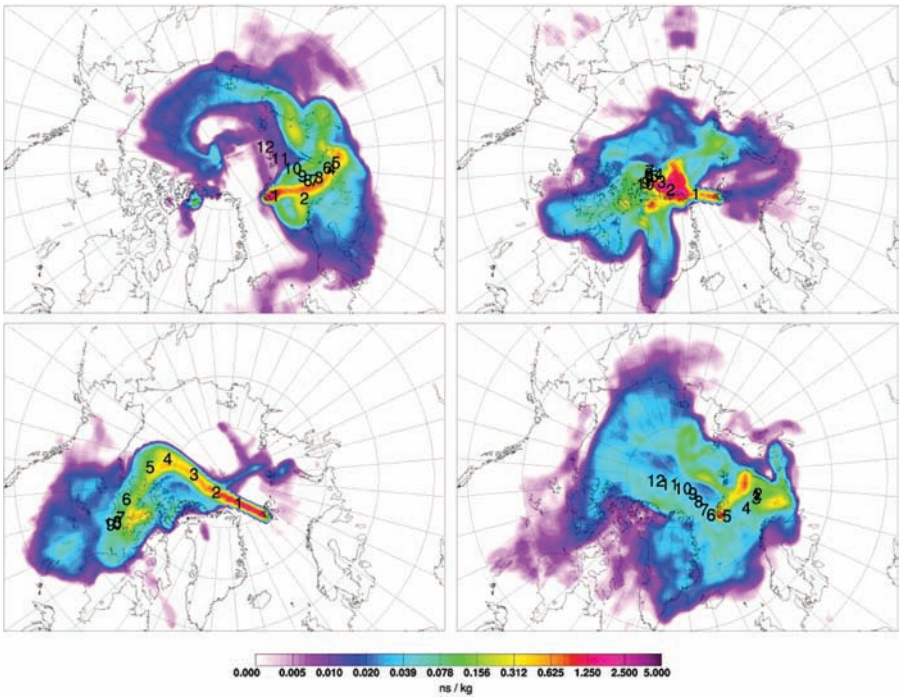

Fig. 1. Representative FLEXPART images, exemplifying the major differences in pathways and source regions between the sampling dates. Upper left picture represents filters A4-A7 (22–23 May). Upper right-hand side picture represents filters C1, E4–E6 (27 May, 3 June). Lower left-hand side picture represents filters G1, G4, H4, H5 (7, 8 and 11 June). Lower right-hand side picture represents filter J1 (14 June) (Warmer colour—higher contribution; numbers stand for days past until arrival).

(27 May) to the area north of Greenland (3 June), that can be seen in the upper right-hand side picture in Fig. 1.

(3) **7 June** (G1), **8 June** (G4), **11 June** (H4, H5), lower left-hand side picture, Fig. 1.

For 7 and 8 **June**, the main source region is a narrow band, stretching over the western Arctic Ocean, and down over Northern Canada, so the air is travelling mostly over ice-covered areas. The only continent that could have recently affected the sampling is North America. For 11 June, FLEXPART shows the source region to be almost identical to previous days, but the main uptake area is now in Svalbards closest surroundings.

(4) **14 June** (J1), lower right-hand side picture, Fig. 1.

On this day, the source region covers practically the whole Arctic Ocean, and includes Greenland, Northern Canada, Northern Siberia and the North Atlantic Ocean. The main source region is concentrated to Svalbards absolute surroundings and to Barents Sea. At the same time, the age spectrum for the trace gases SO_2, NO_2 and CO, show a contribution, approximately older than 2 weeks, from Europe for all gases on this particular day.

3.3. Filter contents

One of the main scopes of this study was to investigate possible differences in aerosol composition between clear sky and cloudy conditions. Three occasions where filters were sampled in succession, first prior to a cloud event and then during the cloud event were identified. These six filters were exposed: 22 and 23 May (A6, A7); 3 June (E5, E6) and 11 June (H4, H5). When comparing the chemical composition before and in cloud for the three occasions, no systematic difference could be found, so no defensible conclusion can be drawn from this comparison. Thus, for the following analysis we no longer distinguish between clear sky and cloud samples.

(1) **A4, A5, A6, A7** (22 and 23 May)

As can be seen in Fig. 2, the four samples collected during this period are very similar and strikingly different from samples collected later during the observation period. More than 80% of the particles were of undefined-organic nature. In contrast to other samples, with many supermicron particles, almost all particles were in the size interval 0.1–0.6 μm, and of spherical shape. Almost all of the remaining 20% of the particles were also of undefined-organic nature, but with trace amount of sulphur. This indicates certain degree of cloud processing during transport. For these filters, the number density of identical particles was high, and the counting procedure described above was applied.

(2) **C1** (27 May)

Only 2% of the particles could be characterized as 'Undefined-Organic smooth', which is a huge difference from the previous filters. The majority of the particles were irregular and in the submicrometre range. Forty-seven per cent of the particles were

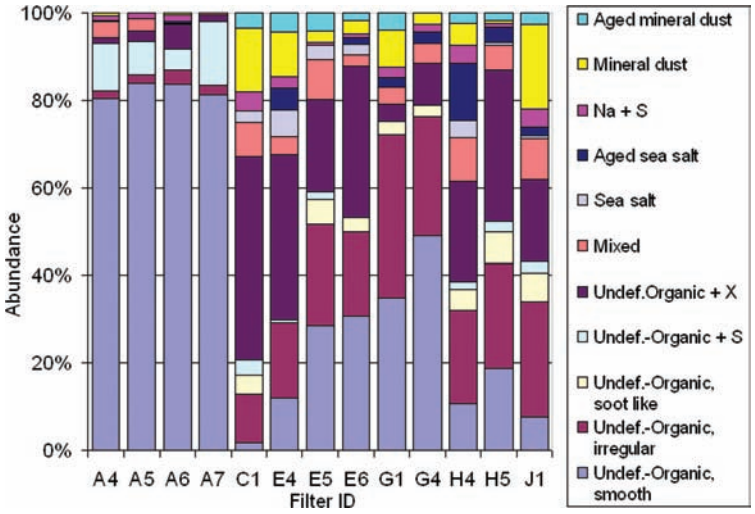

Fig. 2. Particle group relative abundance (%) for analysed filters sampled between 22 May and 14 June.

of 'Undefined-Organic + X' character. Their origin is unclear since they can be biogenic, from land or ocean or the result of in-cloud processes. Surprisingly, considering the source region to be the closest surroundings to Svalbard, where there is open water, no pure or aged sea salt particles were found, only 3% 'Na' and 4% 'Na + S' particles were found. This might be due to the fact that the wind speeds were low and the oceanic source was weak. Instead, the aerosols retained more of a continental characteristic and as much as 15% of the analysed particles were mineral dust.

(3) **E4, E5, E6** (3 June)

The major difference between these three samples, is in the fraction of undefined-organic dominated particles. This group increases from 67% (E4) to 87% (E6). The 'Undefined-Organic smooth' group increases from 12% (E4) to 30% (E6), and most of them are elliptical, in contrast to the spherical ones on filters A4–A7. Also the submicrometre particle fraction increases from filter E4 (77%) to E6 (91%). There are also changes within the group 'Undefined-Organic + X'. This group goes from being dominated by particles carrying S to being dominated by particles without it. When it comes to 'Sea salt', 'Aged sea salt' and 'Na + S' particles, their abundance decreases despite the increase of the height of the atmospheric boundary layer (information from FLEXPART data not shown) and potential increase of a contribution from open water areas. This is probably due to the enhanced cloudiness during the period, since sea salt particles preferably become activated into cloud condensation nuclei. Also the decrease in 'Aged mineral dust', from filter E4 to E6, can be linked to the cloudiness.

(4) **G1** (7 June)

The 'Undefined-Organic + X' group was small on this filter, only 4%, same amount as for the 'Mixed' group. The 'pure' undefined-organic particles were dominating, 35% were 'Undefined-Organic smooth' (the amount of spherical and elliptical were 34 and 11, respectively), and 40% were 'Undefined-Organic irregular' (including soot like). There were no 'Sea salt' particles, and the 'Aged sea salt' and 'Na + S' groups made up 2% each, of the total particle number. 'Mineral dust' contributed with 9% and 'Aged mineral dust' with 4%.

(5) **G4** (8 June)

Almost half (49%) of all the particles found on this filter were 'Undefined-Organic smooth', divided into 33 spherical and 23 elliptical. Another 30% were 'Undefined-Organic irregular' (including soot like). The fraction of 'Undefined-Organic + X' particles was up to 10%. There was no 'Aged mineral dust' and the group 'Mineral dust' was down to 3%. There were only small changes within the groups 'Mixed', 'Aged mineral dust' and 'Na + S' compared with previous day.

(6) **H4, H5** (11 June)

Compared with the other filters, the amount of undefined-organic dominated particles is low, only 61%, on the H4-filter. Also, the rather high presence of 'Aged sea salt', 13%, distinguishes this filter from the others. For the H5 filter, the undefined-organic dominated group is back to high fraction (87%). The soot like group makes up for 7% of those, which is the highest value of all the filters. The 'Aged mineral' group decreased to 2%, and the 'Sea salt', 'Na + S' and 'Mineral dust' are less than 1% each.

(7) **J1** (14 June)

Despite the fact that the source region includes open water areas, the groups 'Sea salt', 'Aged sea salt' and 'Na + S' only made up for 7% of the particles found on filter J1. This filter had a similar amount of undefined-organic dominated particles (62%) as 11 June, at the same time, a relatively high amount of 'Mineral dust' (19%). The majority of the particles in the groups 'Undefined-Organic + X' and 'Mixed' also included S. Together with 'Undefined-Organic + S', 'Aged sea salt', 'Na + S' and 'Aged mineral dust', 39% of the analysed particles on this filter contained sulphur.

4. Discussion

One of the characteristic features of the Arctic aerosol observed at the Zeppelin station is that the properties and size distribution change rapidly every year during late spring. The spring accumulation mode dominated particle size distribution then shifts to an Aitken mode dominated one during a short period of approximately 2 weeks. The explanation for this transition is, probably, a combination of events and processes as pointed out in a recent study by Engvall et al. (2007). The authors concluded that the transport alone cannot explain the annually repeated transition from spring-type to summer-type aerosol, but it is an important pre-requisite. With a simple model, they further suggest that the increasing nucleation potential for new particle formation is the result of a delicate balance between incoming solar radiation, transport and condensational sink processes, but that the timing is mainly controlled by solar radiation. Therefore, the right conditions will appear around the same time every year.

The ASTAR 2004 campaign period was cleaner than 'normal', and the sampling period for this study did not include any large pollution events. The transition between spring and summer conditions was estimated to have taken place around day 145 of the year (between 23 and 27 May) based on the criteria presented by Engvall et al. (2007). This ratio is essentially a relation between the aerosol condensational sink and the potential production of H_2SO_4 molecules based on the observed daily average of SO_2 and solar radiation. Using the three variables mentioned in the previous sentence, an equilibrium H_2SO_4 concentration can be derived. A ratio of unity means that every day, within a seven-day period, exceeds a particular threshold for the equilibrium H_2SO_4 concentration. This sulphuric acid threshold condition was used in Engvall et al. (2007) in trying to understand the rapid shift in the observed size distributions. This threshold ratio or particle nucleation potential, which defined the transition period, is presented in Fig. 3 for an equilibrium H_2SO_4 value of 1.1×10^7 cm^{-3} together with arrows indicating when the different samples were collected. This way, we may compare how the transition in the particle nucleation potential relates to the change in chemical composition over the sampling period. As the analytical technique used in this study only detects particles larger than approximately 0.1 μm in diameter, which bias the data towards mass rather than number concentration, we also included the aerosol mass concentration in Fig. 3. The mass concentration is derived from the observed aerosol size distribution assuming a particle density of 1.5 g cm^{-3}. To harmonize the data, the mass concentration is filtered using a 1-week moving average. We note that although the magnitude of the ratio increases rapidly between day 140 and day 150, the aerosol mass concentration presents three major oscillations while gradually decreasing from spring to summer. In Fig. 2, this transition takes place between sampling of filter A7 and C1, (for details concerning the exposure times, see Table 2).

The main difference between the filters collected on the 22 and 23 May compared with the samples collected 27 May and onwards is in the relative abundance of the 'Undefined-Organic smooth' group. There is still a large abundance of undefined-organic particles even on filters C1 and later, but other groups become more pronounced. We note that the fraction of the 'Undefined-Organic + X' and 'Undefined-Organic irregular' groups increases as the 'Undefined-Organic smooth' group is reduced. At the same time, we note the appearance of several minor groups such as the 'Undefined-Organic soot like' and 'Mineral dust' groups. The 'Undefined-Organic soot like' particles can be both of natural and of anthropogenic origin, but this group and the mineral groups are evidence of a continental influence on the air mass. At the same time the relative influence of marine groups also increase. Even in late spring and early summer, most of Svalbard is still covered by ice and snow. It is unlikely that Svalbard would be a large contributor to mineral dust on the samples. It can, of course, not be excluded that some snow free areas close

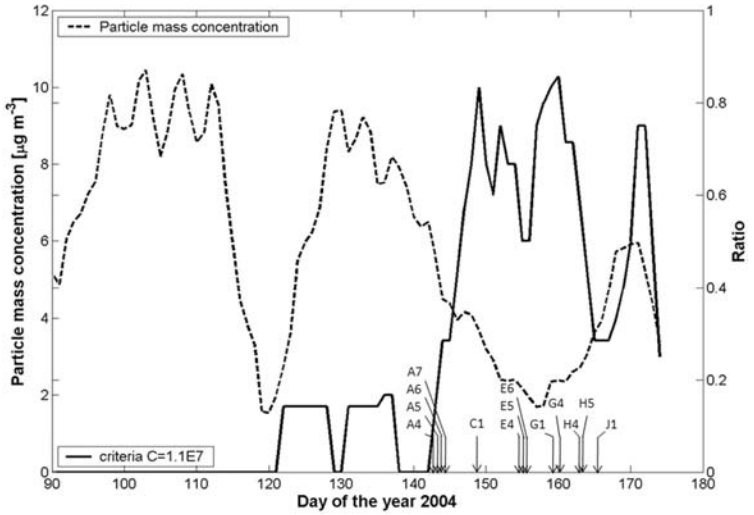

Fig. 3. Aerosol particle mass concentration and the ratio of days exceeding the equilibrium H_2SO_4 concentration of 1.1×10^7 cm^{-3}, using a 7 d running mean over the period April–June 2004. The transition from spring to summer period takes place around DOY 145, based on the ratio criteria proposed by Engvall et al. (2007).

Table 2. Abundance of the eight aerosol particle groups ±1 *SD* for the analysed particles on each filter

Sampling date	Time on/off (UTC)	Filter ID.	Number of particles analysed	Abundance in % (± *SD*)							
				Mineral dust	Aged mineral dust	Sea salt	Aged sea salt	Undefined-Organic	Undefined-Organic + S	Undefined-Organic + X	Mixed
22 May	11:04–17:04	A4	63	0	3.2 ± 2.2	1.6 ± 1.6	6.3 ± 3.1	31.7 ± 5.9	28.6 ± 5.7	7.9 ± 3.4	20.6 ± 5.1
	17:04–23:04	A5	34	0	0	0	8.8 ± 4.7	26.5 ± 7.6	26.5 ± 7.6	17.6 ± 6.5	20.6 ± 6.9
23 May	23:04[a]–05:04	A6	87	0	1.1 ± 1.1	1.1 ± 1.1	8.0 ± 2.9	49.4 ± 5.4	18.4 ± 4.2	21.8 ± 4.4	0
	05:04–11:04	A7	72	0	0	0	0	45.8 ± 5.9	38.9 ± 5.7	12.5 ± 3.8	2.8 ± 1.9
27 May	15:37–21:37	C1	116	3.4 ± 1.7	14.7 ± 3.3	2.6 ± 1.5	4.3 ± 1.9	17.2 ± 3.5	3.4 ± 1.7	46.6 ± 4.6	7.8 ± 2.5
3 June	09:39–15:39	E4	117	4.3 ± 1.9	10.3 ± 2.8	6.0 ± 2.2	7.7 ± 2.5	29.1 ± 4.2	0.9 ± 0.9	37.6 ± 4.5	4.3 ± 1.9
	15:39–21:39	E5	122	4.1 ± 1.8	2.5 ± 1.4	3.3 ± 1.6	0.8 ± 0.8	57.4 ± 4.5	1.6 ± 1.1	21.3 ± 3.7	9.0 ± 2.6
	21:39–03:39[b]	E6	124	1.6 ± 1.1	3.2 ± 1.6	2.4 ± 1.4	2.4 ± 1.4	53.2 ± 4.5	0	34.7 ± 4.3	2.4 ± 1.4
7 June	14:30–20:30	G1	129	3.9 ± 1.7	8.5 ± 2.5	0	4.7 ± 1.9	75.2 ± 3.8	0	3.9 ± 1.7	3.9 ± 1.7
8 June	08:30–14:30	G4	114	0	2.6 ± 1.5	0	4.4 ± 1.9	78.9 ± 3.8	0	9.6 ± 2.8	4.4 ± 1.9
11 June	05:04–11:04	H4	122	2.5 ± 1.4	4.9 ± 2.0	4.1 ± 1.8	17.2 ± 3.4	36.9 ± 4.4	1.6 ± 1.1	23.0 ± 3.8	9.8 ± 2.7
	11:04.17:04	H5	122	1.6 ± 1.1	0.8 ± 0.8	0.8 ± 0.8	4.1 ± 1.8	50.0 ± 4.5	2.5 ± 1.4	34.4 ± 4.3	5.7 ± 2.1
14 June	09:06–15:06	J1	118	2.5 ± 1.4	19.5 ± 3.6	0.8 ± 0.8	5.9 ± 2.2	40.7 ± 4.5	2.5 ± 1.4	18.6 ± 3.6	9.3 ± 2.7

Note: In the text, abundances presented in this table have been rounded to integer percentages.

[a]Start on 22 May.

[b]End on 4 June.

to the station potentially could be a source of mineral particles. However, the period of sampling was characterized by low wind speeds, and the mineral particles observed on our filters are most likely a result of long-range transport.

The FLEXPART simulations indicate a more near-field Arctic influence on the source contributions after the transition. Although, large areas of the Arctic are still ice covered in May and June, the increased Marine component ('Sea salt' and 'Aged sea salt' groups) is clearly possible as there are open oceans around and, in particular, south of Svalbard. Especially the 'Undefined-Organic irregular' group may be a result of direct biogenic ocean particle production taking place near the ocean surface as discussed by Nilsson et al. (2001) and Leck and Bigg et al. (2005). Nonetheless, the samples retain traces of continental character at the same time as the whole signature becomes more complex, with a larger abundance of mixed particles post-transition.

When the transport of air masses into the Arctic from lower latitudes becomes suppressed during summer, the air is circulating within the Arctic region for a long time. During this period, original chemical signatures of the air masses (continental, biogenic or anthropogenic) are modified by natural sources within the Arctic as well as by sink processes. Thus, even if the station is in cloud-free air during sampling, precipitating clouds upstream of the station will selectively have scavenged the more hygroscopic particles. This could be offered as an explanation for the reduced abundance of the possible hygroscopic groups 'Aged mineral' and 'Undefined-Organic + S' and the enhanced abundance of the likely less hydroscopic groups 'Undefined-Organic soot like' and 'Mineral dust' and give the post-transition samples their complex chemical signature and the appearance of coming from a combination of different sources. Note that the hygroscopic nature of these different particles types are not known from this study, and the selective scavenging by clouds is only offered as a possible explanation for the observed change in chemical composition with time.

The measured particle number densities, for aerosol diameter larger than 0.1 μm, averaged over the sampling period of the different filters, presented in Fig. 4, also show a reduction over the studied period, consistent with the overall reduction of accumulation mode particles post-transition. Besides filter H5, a further reduction in the accumulation number density appeared when the sampling was conducted in clouds. As pointed out above, a clear difference in the chemical characterization could not be distinguished between non-cloud and cloud influenced samples taken in succession. One reason for this may be that clouds are not present at all times even if a sample is flagged as being influenced by clouds. Over the 6 h that the filters are exposed, periods of non-cloudy air may have a strong influence on the chemical signature of the sample. This is simply due to the fact that the non-cloudy air contains a higher number density of accumulation mode particles and hence, is ascribed a greater weight.

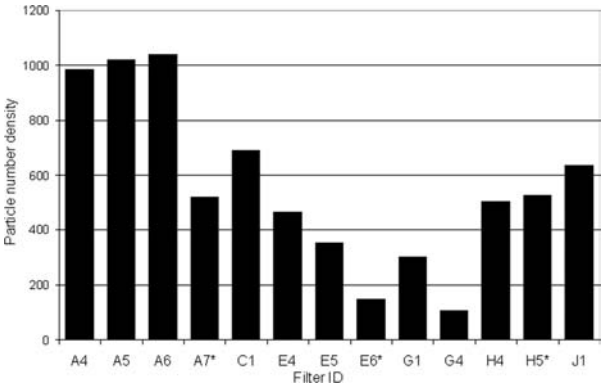

Fig. 4. Average number density (cm^{-3}) of particles larger than 100 nm diameter for the time intervals corresponding to the analysed filters. Filter id with '$*$' indicate that a major part of the time the sampling was in cloudy conditions.

As mentioned before, the sampling period was cleaner, compared to the same period for other years, with no large pollution events. 22 and 23 May is a rather isolated event with high particle number density.

5. Summary and conclusions

Despite the limited number of samples, a difference in chemical signature could be observed between filters exposed during the spring vs. those exposed during the summer period, as defined by Engvall et al. (2007). About nine of ten particles analysed on the spring samples were composed of spherical undefined-organic particles, with or without S on the particles. The summer samples show a large fraction of undefined-organic type particles as well, but several new particle types appear. The fractions of irregular 'pure' undefined-organic particles and undefined-organic, with small addition of element(s), increases whereas the fraction of spherical undefined-organic particles decreases.

Interestingly, summer samples present enhanced abundance of particles associated with both marine as well as continental sources. Hence, even if the numerical transport simulations indicate the Arctic as the main source region, the samples retain or acquire some continental signature (15–25% of the particles).

Our material did not allow for an unambiguous comparison between samples collected in cloudy and non-cloudy air. However, the summer samples presented, enhanced abundance of 'Undefined-Organic soot like' and 'Mineral' groups compared with the spring samples. Precipitation scavenging by the extensive Arctic stratus clouds in the summer time could give rise to such signature.

6. Acknowledgments

The authors would like to acknowledge the financial support by the Swedish Environmental Protection agency and the

Stockholm University Climate Research Environment (SUCLIM) programme at Stockholm University. AS was supported by the Norwegian Research Council in the framework of POLARCAT. Also, thanks to the engineers of the Norwegian Polar Institute for helping out with the equipment at the Zeppelin station. Thanks to Ann-Christine Engvall for her help with data handling and figures. Thanks to the staff at the Department of Geology and Geochemistry, Stockholm University for help with the SEM equipment. The authors acknowledge support by the Nordic Centre of Excellence, BACCI.

References

ACIA 2005. *Arctic Climate Impact Assessment 2005*. Cambridge University Press, Cambridge, UK, 1042p.

Adams, J. W. and Cox, R. A. 2002. Halogen chemistry of the marine boundary layer. *J. Phys. IV France* **12**, 105–124.

Baraskan, M. and Shaw, G. E. 2001. Residence time of Arctic haze aerosols using the concentrations and activity ratios of ^{210}Po, ^{210}Pb and ^{7}Be. *Aerosol. Sci.* **32**, 443–452.

Beine, H. J. 1999. Measurements of CO in the high Arctic. *Global Change Sci.* **1**, 145–151

Charlson, R. J., Schwartz, J. M., Hales, J. M., Cess, J. A., Coakley, J. A. J., and co-authors. 1992. Climate forcing by anthropogenic aerosols. *Science* **255**, 423–430.

Ebert, M., Weinbruch, S., Hoffman, P. and Ortner, H. M. 2000. Chemical characterization of North Sea aerosol particles. *J. Aerosol. Sci.* **31**, 613–632.

Eneroth, K., Kjellström, E. and Holmén, K. 2003. A trajektory climatology for Svalbard; investigating how atmospheric flow patterns influence observed tracer concentrations. *Phys. Chem. Earth* **28**, 1191–1203.

Engvall, A.-C., Krejci, K., Ström, J., Treffeisen, R., Scheele, R. and co-authors. 2007. Changes in aerosol properties during spring-summer period in the Arctic troposphere. *Atmos. Chem. Phys. Discuss.* **7**, 1215–1260.

Heintzenberg, J. and Larssen, S. 1983. SO_2 and SO_4 in the Arctic: interpretation of observations at three Norwegian arctic-subarctic stations. *Tellus* **35B**, 255–265.

Koch, D. and Hansen, J. 2005. Distant origins of Arctic black carbon: a Goddard Institute for Space Studies ModelE experiment. *J. Geophys. Res.* **110**, D04204, doi:10.1029/2004JD005296.

Krejci, R., Ström, J., de Reus, M. and Sahle, W. 2005. Single particle analysis of the accumulation mode aerosol over the northeast Amazonian tropical rain forest, Surinam, South America. *Atmos. Chem. Phys.* **5**, 3331–3344.

Leck, C. and Bigg, K. 2005. Biogenic particles in the surface microlayer and overlaying atmosphere in the central Arctic Ocean during summer. *Tellus* **57B**, 305–316.

Liljequist, G. H. 1970. *Klimatologi*. Generalstabens Litografiska Anstalt, Stockholm.

Mamane, Y. and Noll, K. E. 1985. Characterization of large particles at a rural site in the eastern United States: mass distribution and individual particle analysis. *Atmos. Environ.* **19**, 611–622.

Mitchell, J. M. 1957. Visual range in the polar regions with particular reference to the Alaskan Arctic. *J. Atmos. Terr. Phys. Spec. Suppl.* 195–211.

Nilsson, E. D., Rannik, Ü., Swietlicki, E., Leck, C., Aalto, P. P. and co-authors. 2001. Turbulent aerosol fluxes over the Arctic Ocean. Part 2: wind driven sources from the sea. *J. Geophys. Res.(D Atmos)* **106**, 32 139–32 154.

Olivier, J. G. J. and Berdowski, J. J. M. 2001. Global emissions sources and sinks. In: *The Climate System*, pp. 33–78. (eds.J. Berdowski, R. Guicherit and B. J. Heij) A.A. Balkema Publishers/Swets & Zeitlinger Publishers, Lisse, The Netherlands. ISBN 90-5809-255-0.

Quinn, P., Miller, T., Bates, T., Ogren, J. A., Andrews, E. and co-authors. 2002. A 3-year record simultaneously measured aerosol chemical and optical properties at Barrow, Alaska. *J. Geophys. Res.* **107**(D11), 4130, doi:10.1029/2001JD001248.

Rosenfeld, D. 2000. Suppression of rain and snow by urban and industrial air pollution. *Science* **287**, 1793–1796.

Sirois, A. and Barrie, L. A. 1999. Arctic lower tropospheric aerosol trends and composition at Alert, Canada. *J. Geophys. Res.* **104**, 11 599–11 618.

Stohl, A. 2006. Characteristics of atmospheric transport into the Arctic troposphere. *J. Geophys. Res.* **111**, D11306, doi:10.1029/2005JD006888.

Stohl, A., Hittenberger, M. and Wotawa, G. 1998. Validation of the Lagrangian particle dispersion model FLEXPART against large scale tracer experiment data. *Atmos. Environ.* **32**, 4245–4264.

Stohl, A., Forster, C., Frank, A., Seibert, P. and Wotawa, G. 2005. Technical note: the Lagrangian particle dispersion model FLEXPART version 6.2. *Atmos. Chem. Phys.* **5**, 2461–2474.

Ström, J., Umegård, J., Tørseth, K., Tunved, P., Hansson, H.-C. and co-authors. 2003. One year of particle size distribution and aerosol chemical composition measurements at the Zeppelin Station, Svalbard, March 2000-March 2001. *Phys. Chem. Earth* **28**, 1181–1190.

Targino, A. C., Krejci, R., Noone, K. J. and Glantz, P. 2006. Single particle analysis of ice crystal residuals observed in orographic wave clouds over Scandinavia during INTACC experiment. *Atmos. Chem. Phys.* **6**, 1977–1990.

Xhoffer, C., Bernard, P. and van Grieken, R. 1991. Chemical characterization and source apportionment of individual aerosol particles over the North Sea and English Channel using multivariate techniques. *Environ. Sci. Technol.* **25**, 1470–1478.